ISSN 1674-1056
http://cpb.iphy.ac.cn
http://iopscience.iop.org/cpb
中国物理 B
Chinese Physics
中国物理
Chinese Physics B

Performance of n-type silicon/silver composite anode material in lithium ion batteries: A study on effect of work function matching degree

Guo-Jun Xu(徐国军), Chen-Xin Jin(金晨鑫), Kai-Jie Kong(孔凯捷), Xi-Xi Yang(杨西西), Zhi-Hao Yue(岳之浩), Xiao-Min Li(李晓敏), Fu-Gen Sun(孙福根), Hai-Bin Huang(黄海宾), Lang Zhou(周浪)

Citation: Chin. Phys. B . 2018, 27(10): 108201. **doi:** 10.1088/1674-1056/27/10/108201

Journal homepage: http://cpb.iphy.ac.cn; http://iopscience.iop.org/cpb

What follows is a list of articles you may be interested in

Size effect of Si particles on the electrochemical performances of Si/C composite anodes

Bonan Liu(刘柏男), Hao Lu(陆浩), Geng Chu(褚赓), Fei Luo(罗飞), Jieyun Zheng(郑杰允), Shimou Chen(陈仕谋), Hong Li(李泓)
Chin. Phys. B . 2018, 27(8): 088201. **doi:** 10.1088/1674-1056/27/8/088201

Improved electrochemical performances of high voltage $LiCoO_2$ with tungsten doping

Jie-Nan Zhang(张杰男), Qing-Hao Li(李庆浩), Quan Li(李泉), Xi-Qian Yu(禹习谦), Hong Li(李泓)
Chin. Phys. B . 2018, 27(8): 088202. **doi:** 10.1088/1674-1056/27/8/088202

Gas treatment protection of metallic lithium anode

Wen-jun Li(李文俊), Quan Li(李泉), Jie Huang(黄杰), Jia-yue Peng(彭佳悦), Geng Chu(褚赓), Ya-xiang Lu(陆雅翔), Jie-yun Zheng(郑杰允), Hong Li(李泓)
Chin. Phys. B . 2017, 26(8): 088202. **doi:** 10.1088/1674-1056/26/8/088202

Conductivity and applications of Li-biphenyl-1, 2-dimethoxyethane solution for lithium ion batteries

Geng Chu(褚赓), Bo-Nan Liu(刘柏男), Fei Luo(罗飞), Wen-Jun Li(李文俊), Hao Lu(陆浩), Li-Quan Chen(陈立泉), Hong Li(李泓)
Chin. Phys. B . 2017, 26(7): 078201. **doi:** 10.1088/1674-1056/26/7/078201

Instability of lithium bis(fluorosulfonyl)imide (LiFSI)–potassium bis(fluorosulfonyl)imide (KFSI) system with $LiCoO_2$ at high voltage

Zhang Shu, Li Wen-Jun, Ling Shi-Gang, Li Hong, Zhou Zhi-Bin, Chen Li-Quan
Chin. Phys. B . 2015, 24(7): 078201. **doi:** 10.1088/1674-1056/24/7/078201

Performance of n-type silicon/silver composite anode material in lithium ion batteries: A study on effect of work function matching degree*

Guo-Jun Xu(徐国军), Chen-Xin Jin(金晨鑫), Kai-Jie Kong(孔凯捷), Xi-Xi Yang(杨西西), Zhi-Hao Yue(岳之浩)†, Xiao-Min Li(李晓敏), Fu-Gen Sun(孙福根), Hai-Bin Huang(黄海宾), and Lang Zhou(周浪)

Institute of Photovoltaics, Nanchang University, Nanchang 330031, *China*

(Received 26 June 2018; revised manuscript received 23 July 2018; published online 27 September 2018)

In this paper, two types of silicon (Si) particles ball-milled from n-type Si wafers, respectively, with resistivity values of 1 Ω·cm and 0.001 Ω·cm are deposited with silver (Ag). The Ag-deposited n-type 1-Ω·cm Si particles (n1-Ag) and Ag-deposited n-type 0.001-Ω·cm Si particles (n0.001-Ag) are separately used as an anode material to assemble coin cells, of which the electrochemical performances are investigated. For the matching of work function between n-type 1-Ω·cm Si (n1) and Ag, n1-Ag shows discharge specific capacity of up to 683 mAh·g^{-1} at a current density of 8.4 A·g^{-1}, which is 40% higher than that of n0.001-Ag. Furthermore, the resistivity of n1-Ag is lower than half that of n0.001-Ag. Due to the mismatch of work function between n-type 0.001-Ω·cm Si (n0.001) and Ag, the discharge specific capacity of n0.001-Ag is 250.2 mAh·g^{-1} lower than that of n1-Ag after 100 cycles.

Keywords: lithium ion battery, silicon anode materials, work function matching, contacts

PACS: 82.47.Aa, 82.45.Fk, 65.40.gh, 73.40.Cg **DOI:** 10.1088/1674-1056/27/10/108201

1. Introduction

With the advent of portable intelligent devices and electric vehicles, the demand of lithium ion batteries (LIBs) with high energy density is growing.[1–4] Due to the high theoretical specific capacity of 4200 mAh·g^{-1}, silicon (Si) anode materials receive more and more attention.[5,6] However, both huge volume expansion effect in the charge-discharge process and poor conductivity of Si anode material restrict its application.[7,8]

In order to improve the conductivity of Si anode material, most of researchers used the technology of metal modification on the surface of Si material,[9–21] especially silver (Ag) modification.[14–21] However, these researches overlook an important fact that Si is a semiconductor material. As Si contacts metallic materials, the contact resistance depends on the matching degree of work functions between Si and metal.[22–24] In the case of a mismatch of work function between Si and metal, a Schottky barrier will be generated between the two, which will result in a rise of contact resistance and ultimately affect the electrochemical performance of metal-modified Si anode material in LIB. In order to clarify the above phenomenon, in this work adopted is a combination of theory and experiment to analyze and verify the problem mentioned above.

In our previous work,[25] we have prepared the Ag-deposited p-type Si particles. However, there is no obvious difference in work function matching degree between Ag and p-type Si with different resistivity values. On the contrary, the work function of Ag is lower than that of n-type 1-Ω·cm-Si particles and higher than that of n-type 0.001-Ω·cm-Si particles. Therefore, the electrochemical performances of the above two kinds of n-type Si particles deposited with Ag as anode materials in LIBs are investigated in this work for clarifying the effect of work function matching degree between Si and metal on their performance in LIB. To the best of our knowledge, the work function matching degree between Si and metal is considered in LIBs for the first time.

2. Experiment

2.1. Ag modification of Si particles

The n-type Si wafers, respectively, with electrical resistivity values of 1 Ω·cm and 0.001 Ω·cm used in this work were purchased from Hangzhou JingBo technology co., LTD. After being ball-milled at 400 rpm for 20 h (SFM-1, Hefei KeJing Materials Technology Co., LTD), Si wafers were refined into submicron Si particles. In our previous work,[25] p-type Si particles were deposited with Ag via self-selective electroless deposition. Hence, we use the same method to prepare Ag-deposited n-type Si particles. After being cleaned by hydrofluoric acid (HF) solution with a volume ratio of 3%, 3-g Si particles were, respectively, reacted with 3-M HF and 17-mM silver nitrate ($AgNO_3$) in a 300-mL solution for 5 min. In the process, 200-mL H_2O was first added to disperse Si particles, and the remaining mixed solution was replenished 3 min later. After being filtrated and washed with H_2O, the Ag-deposited n-type Si particles were dried under vacuum at 40 °C for 4 h.

*Project supported by the China Postdoctoral Science Foundation (Grant No. 2016M592115), the Jiangxi Postdoctoral Foundation, China (Grant No. 2015KY12), the Fund from the Jiangxi Provincial Education Department, China (Grant No. 150184), and the Fund from Nanchang University, China (Grant No. CX2017006).

†Corresponding author. E-mail: yuezhihao@ncu.edu.cn

© 2018 Chinese Physical Society and IOP Publishing Ltd

2.2. Material characterization

Scanning electron microscopy micrographs (SEM) were captured on JEOL JSM-6701 F at 15-kV accelerating voltage. The energy dispersive spectrum (EDS) was obtained from the energy dispersive spectrometer equipped with FE-SEM. Inductively coupled plasma atomic emission spectrometry (ICP-AES, PE Optima8000) was employed to measure the mass content of Ag. Laser diffraction instrument (BT-9300 H, Liaoning, China) was used to measure the sizes of Ag-deposited n-type Si particles. Powder x-ray diffraction (XRD) was obtained by Bruker D8 Advance x-ray diffractometer with using the Cu $K\alpha$ radiation in steps of 0.04° s^{-1}. The electrical resistivity values of the four samples were measured on a semiconductor powder electrical resistivity tester (ST2722, Beijing, China).

2.3. Electrochemical measurements

The anode materials were slurry-cast on copper current collectors. Specifically, Ag-deposited Si particles, super-P and sodium alginate were ground in weight ratio of 7:1.5:1.5, then the as-prepared mixtures with 6-ml H_2O and 2-ml absolute ethanol (C_2H_5OH) were stirred to form slurries. All slurries were coated on copper current collectors, then dried under vacuum at 120 °C for 12 h. Finally, CR2025 coin cells containing as-prepared working electrode, diaphragm, electrolyte and lithium tablets as the reference electrode were assembled inside glove box filled with high-purity argon. The diaphragm was a Celgard 2400 sheet with a diameter of 19 mm. The mixture of 1-M $LiPF_6$/EC: DMC ($V : V = 1 : 1$) was used as the electrolyte.

The LAND battery cycler (LAND BT1-10, Shenzhen, China) was employed to measure the galvanostatic charge-discharge properties of the four samples. The potential voltage ranged from 0.01 V to 1.5 V. Electrochemical impedance spectrum (EIS) was recorded by a Princeton Applied Research spectrometer. The frequency ranged from 0.01 kHz to 100 kHz with an alternating current voltage of 10 mV. All the measurements were carried out at 25 °C.

3. Results and discussion

3.1. Material characterization

The Si particles milled from n-type Si wafers, respectively, with an electrical resistivity of 1 Ω·cm and 0.001 Ω·cm are deposited with Ag in the same process. Figures 1(a) and 1(b) show SEM images of Ag-deposited n-type 1-Ω·cm-Si particles (n1-Ag) and Ag-deposited n-type 0.001-Ω·cm-Si particles (n0.001-Ag), respectively. The ellipsoidal particles with dozens of nanometer in size are attributed to Ag nanoparticles, while submicron Si particles exhibit irregular shapes. Obviously, Ag nanoparticles are evenly dispersed on the surfaces of Si particles. The insets in Figs. 1(a) and 1(b) show EDS and ICP results of n1-Ag and n0.001-Ag, respectively. It can be found in the two figures that the mass percent values of Ag in the surface are almost the same. Moreover, there is no significant difference between the overall Ag content of n1-Ag and that of n0.001-Ag, which can be obtained from the ICP results. The XRD patterns of n1-Ag and n0.001-Ag are shown in Fig. 1(c). The characteristic peaks of Si and Ag are clearly identified. In addition, there are no obvious difference between the full widths at half maximum of Ag in n1-Ag and n0.001-Ag, and so is the scenario of Si. It indicates that the crystal structures of Si and Ag in the n1-Ag and n0.001-Ag are the same.

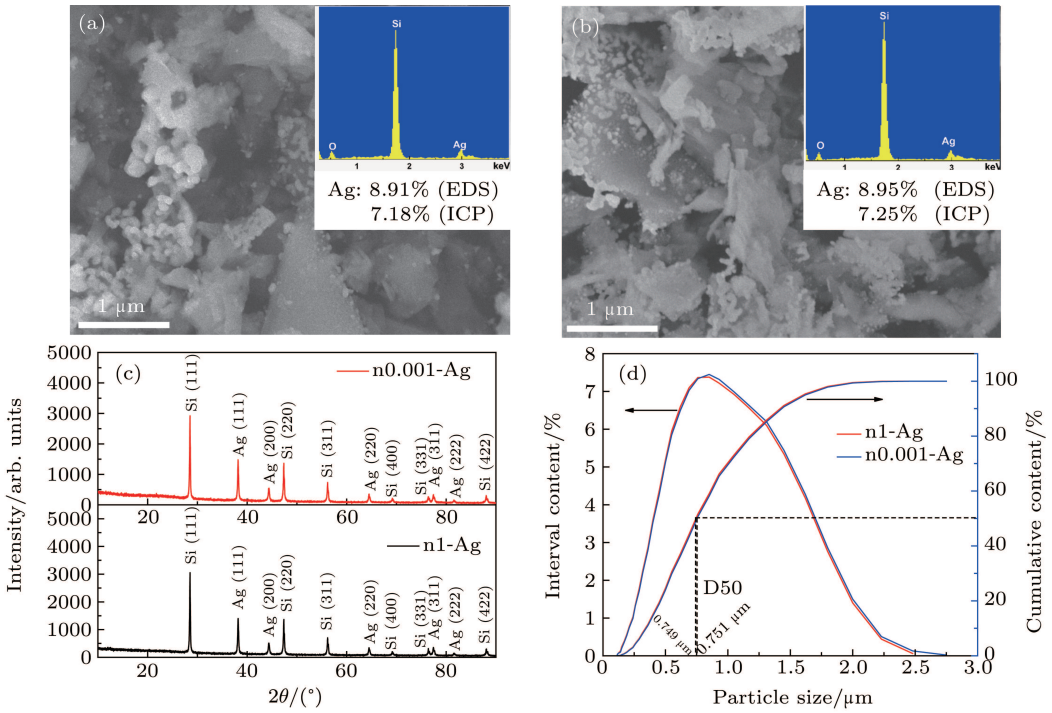


Fig. 1. (color online) SEM images of (a) n1-Ag and (b) n0.001-Ag, (c) x-ray diffraction patterns and (d) particle size distribution curves of n1-Ag and n0.001-Ag.

Figure 1(d) presents that the particle size dispersion curves of n1-Ag and n0.001-Ag. The particle size distribution curves of these two samples basically overlap, which indicates that their particle size is basically the same. Moreover, the median-particle-size D50 of n1-Ag and n0.001-Ag are 0.749 μm and 0.751 μm, respectively. Accordingly, the n1-Ag and n0.001-Ag present similar morphologies, the same crystal structure and undifferentiated size distribution.

3.2. Electrical properties

Figure 2 shows the structural diagram and energy band diagram of n1 and n0.001 before and after being deposited with Ag. Ag, as a metal material, has a work function fixed at 4.26 eV. As a semiconductor material, the work function of Si varies with the type and concentration of doping. In this work, the doping concentration of n-type Si with electrical resistivity of 1 Ω·cm and 0.001 Ω·cm are 4.86×10^{15} cm^{-3} and 7.38×10^{19} cm^{-3}, respectively. It is calculated that the work function of n0.001 ($W_{\mathrm{n0.001}}$) is 4.08 eV, which is 0.18 eV lower than that of Ag.[22] Thus, the energy band of n0.001 is bent downward after deposited with Ag, which generates a Schottky barrier.[22–24] The Schottky barrier causes the contact resistance to rise. On the contrary, the work function of n1 (W_{n1}) is 4.31 eV, which is 0.05 eV higher than that of Ag. After being deposited with Ag, the energy band of n1 is bent upward to reduce the contact resistance. Therefore, the resistivity of n1-Ag is lower than that of n0.001-Ag.

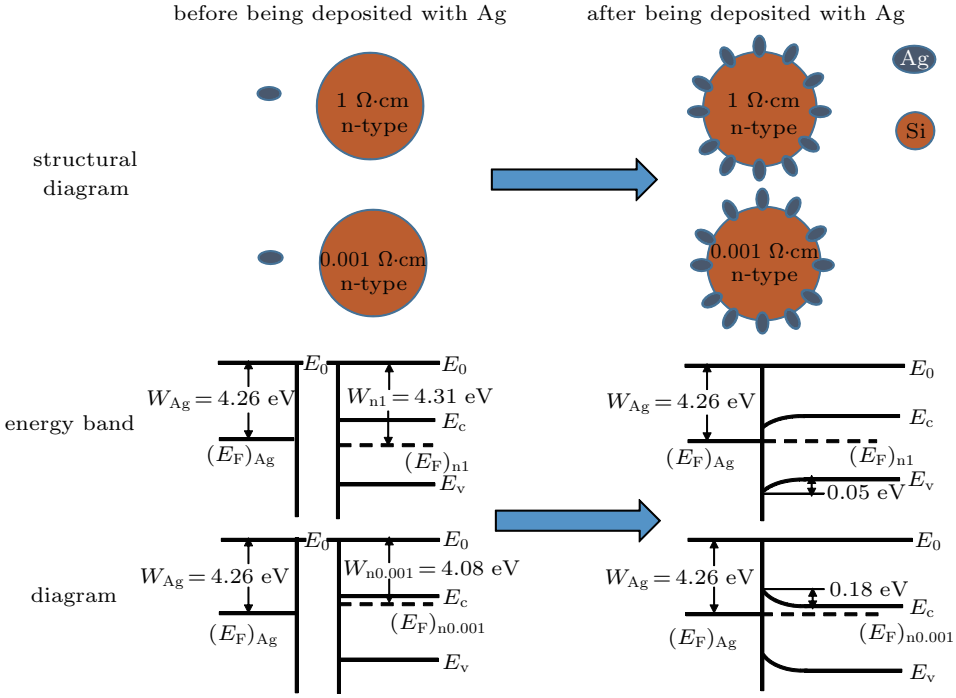


Fig. 2. (color online) Structural diagram and energy band diagram of n1 and n0.001 before and after being deposited with Ag.

The semiconductor powder electrical resistivity tester is used to test the powder resistivity of Si particles and Ag-deposited Si particles in order to characterize their resistivity changes. Powder resistivity values of different samples are shown in Table 1. It can be observed that the powder resistivity of n1 and n0.001 are both several hundred thousand times that of the corresponding Si wafer. This is attributed to the fact that the natural oxide layer on the surface of Si particles increases the contact resistance among them. The powder resistivity values of n1-Ag and n0.001-Ag are 1.11 Ω·cm and 2.49 Ω·cm, respectively, which are lower than that of corresponding Si particles. However, it is worth noting that the powder resistivity of n1-Ag is lower than half that of n0.001-Ag, while that of n1 is 210 times higher than that of n0.001. Specifically, the powder resistivity of n1-Ag is 8.59×10^5 times lower than that of n1, while that of n0.001-Ag is only 1.82×10^3 times lower than that of n0.001. The theoretical analysis mentioned above indicates that the matching of work function between n1 and Ag leads to these results.

Table 1. Powder resistivity of different samples.

Sample	n1	n0.001	n1-Ag	n0.001-Ag
Resistivity	953 kΩ·cm	4.53 kΩ·cm	1.11 Ω·cm	2.49 Ω·cm

3.3. Electrochemical properties

The EIS of the four electrodes are displayed in Fig. 3(a). It can be found that the intercept on x axis in the high frequency region of n1-Ag is smallest. It indicates that n1-Ag has the lowest impedance. It is consistent with the theoreti-

cal analysis mentioned above. Figure 3(b) shows the voltage profiles corresponding to the first cycle of the four electrodes at a current density of 0.42 A·g^{-1}. The discharge specific capacities of n1, n0.001, n1-Ag, and n0.001-Ag in the first cycle are 3139.5 mAh·g^{-1}, 3263.1 mAh·g^{-1}, 2945.1 mAh·g^{-1}, and 2998.2 mAh·g^{-1}, respectively. Due to the presence of Ag, the discharge capacity of Ag-deposited Si particles is lower than that of the corresponding Si particles without Ag, respectively.

Figure 3(c) shows the rate performances of the four types of electrodes at current densities of 0.42 A·g^{-1}, 0.84 A·g^{-1}, 2.1 A·g^{-1}, 4.2 A·g^{-1}, 8.4 A·g^{-1}, and 0.42 A·g^{-1}. Except the first five cycles, the discharge specific capacity of n1-Ag is always highest. In particular, the discharge specific capacity of n1-Ag is 683 mAh·g^{-1} at a current density of 8.4 A·g^{-1}, which is 40% higher than that of n0.001-Ag. The cycle performances of the four types of electrodes are shown in Fig. 3(d). After 100 cycles, the discharge specific capacities of n1, n0.001, n1-Ag, and n0.001-Ag are 682.2 mAh·g^{-1}, 935.1 mAh·g^{-1}, 1401.4 mAh·g^{-1}, and 1151.2 mAh·g^{-1}, respectively. Obviously, the discharge specific capacity of n0.001 is 252.9 mAh·g^{-1} higher than that of n1. This is consistent with our previous result.[26] Dramatically, the discharge specific capacity of n0.001-Ag is 250.2 mAh·g^{-1} lower than that of n1-Ag. This can be attributed to the matching of work function between n1 and Ag, which improves the electrical connection between electrode and active material.

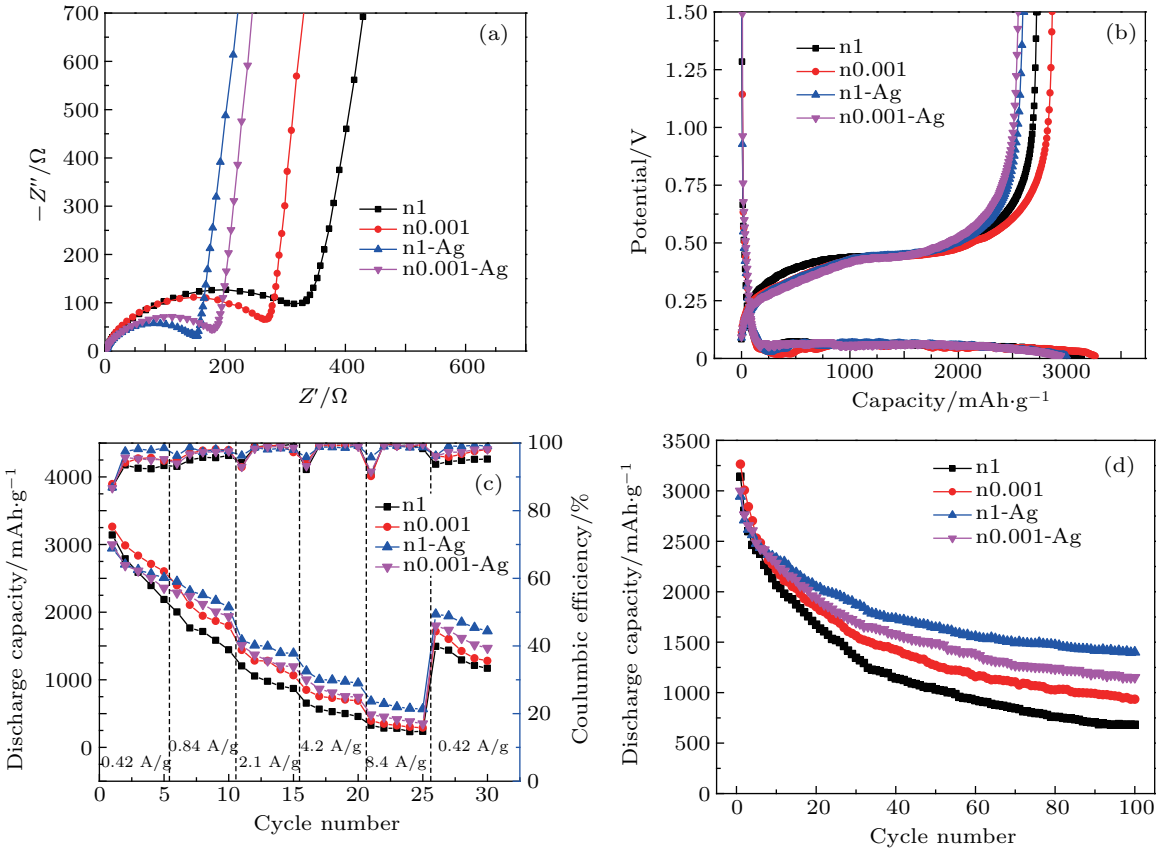


Fig. 3. (color online) (a) EISs of the four electrodes before cycling, (b) the first cycle charge/discharge profiles, (c) rate performance and (d) cyclabilities of four electrodes.

4. Conclusions

In this work, the work function of n1 matches with that of Ag, which results in reducing the contact resistance of n1-Ag, while the contact resistance of n0.001-Ag rises due to the mismatch of work function between n0.001 and Ag. Power resistivity results show that the resistivity of n1-Ag is smallest. The n1-Ag exhibits a promising rate performance with a reversible capacity of 683 mAh·g^{-1} at a current density of 8.4 A·g^{-1}. Moreover, the discharge capacity retention ratio of n1-Ag is higher than that of n0.001-Ag. Therefore, it is necessary to consider the work function matching degree in Si/metal composition material for being used as anode material in LIBs.

References

[1] Zuo X, Zhu J, Müller-Buschbaum P and Cheng Y J 2017 *Nano Energy* **31** 113
[2] Pang H 2017 *Acta Phys. Sin.* **66** 238801 (in Chinese)
[3] Wu M, Xu B and Ouyang C 2016 *Chin. Phys. B* **25** 018206
[4] Y H, Ai L, Jia M, Cheng Y, Du S L and Li S G 2017 *Acta Phys. Sin.* **66** 118202 (in Chinese)
[5] Yamaguchi K, Domi Y, Usui H, Shimizu M, Matsumoto K, Nokami T, Itoh T and Sakaguchi H 2017 *J. Power Sources* **338** 103
[6] Peng Y, Li Y, Zheng B, Zhang K and Xu Y 2018 *Acta Phys. Sin.* **67** 070203 (in Chinese)
[7] Assresahegn B D and Bélanger D 2017 *J. Power Sources* **345** 190

[8] Guo Y, Cao J and Xu B 2016 *Chin. Phys. B* **25** 017101

[9] Memarzadeh E L, Kalisvaart W P, Kohandehghan A, Zahiri B, Holt C M B and Mitlin D 2012 *J. Mater. Chem.* **22** 6655

[10] Murugesan S, Harris J T, Korgel B A and Stevenson K J 2012 *Chem. Mater.* **24** 1306

[11] Yang Z, Wang D, Li F, Yue H, Liu D, Li X, Qiao L and He D 2014 *Mater. Lett.* **117** 58

[12] Huang X H, Zhang P, Wu J B, Lin Y and Guo R Q 2016 *Mater. Res. Bull.* **80** 30

[13] Halim M, Kim J S, Nguyen S H, Jeon B J and Lee J K 2015 *J. Nanosci. Nanotechnol.* **15** 8222

[14] Baek S H, Park J S, Jeong Y M and Kim J H 2016 *J. Alloys Compd.* **660** 387

[15] Yao W, Cui Y, Zhan L, Chen F, Zhang Y, Wang Y and Song Y 2017 *Appl. Surf. Sci.* **425** 614

[16] Talla G, Guduru R K, Li B Q and Mohanty P S 2015 *Solid State Ionics* **269** 8

[17] Hao Q, Zhao D, Duan H, Zhou Q and Xu C 2015 *Nanoscale* **7** 5320

[18] Kwon E, Lim H S, Sun Y K and Suh K D 2013 *Solid State Ionics* **237** 28

[19] Gu M, Ko S, Yoo S, Lee E, Min S H, Park S and Kim B S 2015 *J. Power Sources* **300** 351

[20] Yoo S, Lee J I, Ko S and Park S 2013 *Nano Energy* **2** 1271

[21] Wang Q, Han L, Zhang X, Li J, Zhou X and Lei Z 2016 *Mater. Lett.* **185** 558

[22] Sze S M and Ng K K 2006 *Physics of Semiconductor Devices*, 3rd edn. (Hoboken: John Willey and Sons)

[23] Wolf H F 1971 *Semiconductors* (New York: John Willey and Sons)

[24] Harrison W A, Goebel A and Clifton P A 2013 *Appl. Phys. Lett.* **103** 138

[25] Xu G, Jin C, Liu L, Lan Y, Yue Z, Li X, Sun F, Huang H and Zhou L 2017 *Appl. Phys. A* **123** 752

[26] Yue Z, Zhou L, Jin C, Liu L, Xu G, Tang H, Huang H, Yuan J and Gao C 2017 *Mater. Lett.* **186** 217